Langmuir
Article
pubs.acs.org/Langmuir

Incorporation and Exclusion of Long Chain Alkyl Halides in Fatty Acid Monolayers at the Air−Water Interface

M. Roxana Sierra-Hernández and Heather C. Allen*

Department of Chemistry, The Ohio State University, 100 West 18th Avenue, Columbus, Ohio 43210, United States

Received August 16, 2010. Revised Manuscript Received October 29, 2010

Mixed monolayers of deuterated palmitic acid $C_{15}D_{31}COOH$ (dPA) and deuterated stearic acid $C_{17}D_{35}COOH$ (dSA) with 1-bromoalkanes of different alkyl chain length (C_4 to C_{16}) at the air−water interface were investigated. Alkanes and 1-chlorohexadecane $ClC_{16}H_{33}$ (ClHex) were also studied to compare the effects of the halogen on the mixed monolayers. Surface pressure−area isotherms and Brewster angle microscopy (BAM) were used to obtain the organization and phase behavior, providing a macroscopic view of the mixed monolayers. A molecular-level understanding of the interfacial molecular organization and intermolecular interactions was obtained by using vibrational sum frequency generation (SFG) spectroscopy and infrared reflection−absorption spectroscopy (IRRAS). It was found that from the alkyl halide molecules investigated 1-bromopentadecane, $BrC_{15}H_{31}$ (BrPent), 1-bromohexadecane, $BrC_{16}H_{33}$ (BrHex), and ClHex incorporate into the fatty acid monolayers. Alkanes of 15- and 16-carbon chain length do not incorporate into the fatty acid monolayer, which suggests that the halogen is needed for incorporation. Isotherms and spectra suggest that BrHex molecules are squeezed out, or excluded, from the fatty acid monolayer as the surface pressure is increased, while BAM images confirm this. Additionally, SFG spectra reveal that the alkyl chains of both fatty acids (dPA and dSA) retain an all-trans conformation after the incorporation of alkyl halide molecules. BAM images show that at low surface pressures BrHex does not affect the two-dimensional morphology of the dPA and dSA domains and that BrHex is miscible with dPA and dSA. We also present for the first time BAM images of BrHex deposited on a water surface, which reveal the formation of aggregates while the surface pressure remains unchanged from that of neat water.

Introduction

Aerosols are ubiquitous and have been recognized for years to play an important role in the atmosphere.[1] Gill et al.[2] proposed in 1983 the existence of marine aerosols coated with hydrophobic organic monolayers. These fat-coated aerosols were described as inverse micelles with the polar head of the carboxylic groups of the fatty acids (R−COOH) oriented into the water droplet and the alkyl chains oriented outward. Tervahattu et al.[3,4] found that fat-coated aerosols exist in both marine and continental regions. They found that fatty acids such as palmitic acid (PA) and stearic acid (SA) as well as other acids of alkyl chain length up to the C_{32} covered the surfaces of the marine aerosols.

Such organic films may affect the chemical, physical, and optical properties of aerosol particles, which in turn might have effects on different atmospheric processes. A great number of organic compounds are emitted into the atmosphere from both biogenic and anthropogenic sources; therefore, it is expected that a variety of organics exist within the surface region of atmospheric aerosols. Thus, a fundamental molecular level understanding of the intermolecular interactions and molecular organization of different organic species at air−water surfaces is a natural step to understand the processing of atmospheric aerosols as is discussed here. For this aim, Langmuir monolayers are used as proxies of organic-coated aerosols.

Langmuir monolayers are normally formed by amphiphilic molecules with a hydrophilic headgroup and a hydrophobic chain. The stability of a monolayer depends on the chemical and physical properties of the film. Fatty acids such as PA form stable monolayers at the air−water interface by themselves. Long chain alkyl halides do not form monolayers by themselves; however, they can be incorporated into existing monolayers.[5−7]

A complex array of organics are emitted into the atmosphere; thus, the surfaces of aerosols are expected to have a highly complex composition.[1] Mixed monolayers are therefore more appropriate models to understand aerosol surfaces. Mixed Langmuir monolayers are monomolecular films containing more than one chemical species.[8] In this investigation, mixed monolayers of two fatty acids, deuterated palmitic acid, $C_{15}D_{31}COOH$ (dPA) and deuterated stearic acid, $C_{17}D_{35}COOH$ (dSA), with alkyl halides (1-bromoalkanes) of different carbon chain length and 1-chlorohexadecane at the air−water interface were investigated. Previously, we have investigated fatty acid films[9−11] as have many others.[8,12−18] Palmitic acid and stearic acid were chosen for this

*Corresponding author. E-mail: allen@chemistry.ohio-state.edu.

(1) Finlayson-Pitts, B. J.; Pitts, J. N. J. *Chemistry of the Upper and Lower Atmosphere: Theory, Experiments, and Applications*; Academic Press: San Diego, 2000.
(2) Gill, P. S.; Graedel, T. E.; Weschler, C. J. *Rev. Geophys. Space Phys.* **1983**, *21*, 903.
(3) Tervahattu, H.; Juhanoja, J.; Kupiainen, K. *J. Geophys. Res.* **2002**, *D16*, ACH18/1.
(4) Tervahattu, H.; Juhanoja, J.; Vaida, V.; Tuck, A. F.; Niemi, J. V.; Kupiainen, K.; Kulmala, M.; H. Vehkamäki, H. *J. Geophys. Res.* **2005**, *110*, D06207.
(5) Baskar, G.; Shanmugharaj, A. M.; Venkatesh, S.; Mandal, A. B. *J. Am. Oil Chem. Soc.* **2001**, *78*, 503–507.
(6) Gonçalves da Silva, A. M.; Guerreiro, J. C.; Rodrigues, N. G.; Rodrigues, T. O. *Langmuir* **1996**, *12*, 4442–4448.
(7) Peters, A.; Rogers, K. *J. Colloid Interface Sci.* **1993**, *157*, 511–512.
(8) Gaines, G. L. *Insoluble Monolayers at Liquid-Gas Interfaces*; Interscience Publishers: New York, 1966.
(9) Ma, G.; Allen, H. C. *Langmuir* **2007**, *23*, 589–597.
(10) Tang, C.; Allen, H. C. *J. Phys. Chem. A* **2009**, *113*, 7383–7393.
(11) Voss, L. F.; Hadad, C. M.; Allen, H. C. *J. Phys. Chem. B* **2006**, *110*, 19487–19490.
(12) Adam, N. K. *The Physics and Chemistry of Surfaces*, 3rd ed.; Oxford University Press: London, 1941.
(13) Guyot-Sionnest, P.; Hunt, J. H.; Shen, Y. R. *Phys. Rev. E* **1987**, *59*, 1597–1600.
(14) Henon, S.; Meunier, J. *Rev. Sci. Instrum.* **1991**, *62*, 936–939.

investigation because they have been found in abundance in the organic surface layer of marine aerosols.[3,4] Halogenated organic compounds from both biogenic and anthropogenic sources are emitted into the atmosphere. Of the alkyl halides, short-chain alkyl halides have been found in the atmosphere, in addition to the oxidization products of halogens.[19] Of the alkyl halides, methyl chloride (CH_3Cl),[20,21] methyl bromide (CH_3Br),[1] methyl iodide (CH_3I), ethyl iodide (C_2H_5I), and 1-propyl iodide (C_3H_7I)[22] as well as CH_3CCl_3, CH_2Cl_2, and variations of $CH_xCl_yBr_z$ among others[1,23] have been identified and discussed. Although longer chain alkyl halides have not been identified in the atmosphere, many marine organisms contain significant quantities of brominated organic compounds (BOCs; $\gg C_2$), some of which have anthropogenic origins from bioaccumulation of brominated flame retardants.[24−26] We therefore assert that atmospheric aerosol surface films will also be comprised of these BOCs.

The first step for this investigation was to determine the minimum chain length of alkyl halide that incorporates into dPA and dSA monolayers by conducting surface pressure−area isotherms. For this, alkyl bromide molecules from C_3 to C_{16} chain length were tested. Only C_{15} and C_{16} alkyl bromides spread with dPA and dSA as films revealed a surface pressure change relative to the pure dPA and dSA surfaces. Here we present the thermodynamic and spectroscopic results of dPA and dSA mixed with those alkyl halides that incorporated into the fatty acid monolayer.

This article is organized as follows. Surface pressure−area isotherms are shown to understand the phase behavior and self-organization of mixed monolayers. Vibrational sum frequency generation (SFG) spectroscopy data are presented to understand how the alkyl halide molecules affect the conformations of the fatty acid molecules. Then, IRRAS spectra of two different systems dSA-BrHex (3:1 and 1:1) and dPA-BrHex (3:1 and 1:1) are presented to elucidate further the chain ordering and to track surface number densities. In addition, Brewster angle microscopy (BAM) images are shown to provide an alternate view of the morphological film parameters such as film homogeneity, domain size, shape and packing and to shed further light on miscibility.

Experimental Section

Materials. Deuterated palmitic acid, $C_{15}D_{31}COOH$ (dPA), and deuterated stearic acid, $C_{17}D_{35}COOH$ (dSA), with 98% of purity were obtained from Cambridge Isotope Laboratories, Inc. Alkyl halides (RX) were used as received from Acros Organics without further purification. Solutions of each were prepared in chloroform (> 99.8%, HPLC grade, Fisher Scientific). Monolayers were spread on deionized water with a resistivity of 18.2 MΩ cm (Barnstead Nanopure filtration system). All experiments were conducted at room temperature (22 ± 1 °C) and at atmospheric pressure.

Methods. *Langmuir Film Balance*. Surface pressure−area isotherms were performed with a KSV minitrough (KSV Instruments, Finland). The trough is made of Teflon and has dimensions of 176.5 mm × 85 mm. The film compression was symmetrically performed by two interlinked surface barriers. The barriers are made of Delrin, which prevents leakage of the monolayer under the barriers. The surface pressure and mean molecular area (MMA) were continuously monitored during film compression by the Wilhelmy plate method. Filter paper plates were used (Whatman ashless filter paper # 41). The trough was filled with pure water (Nanopure) as the subphase. The aqueous subphase was replaced after each isotherm measurement. Before spreading the sample on the subphase, the subphase was swept by the barriers to ensure that there was no significant surface pressure increase upon compression. Stock solutions of dPA, dSA, and of each alkyl halide were prepared in chloroform with a concentration of 2 mM. Mixed solutions of dPA−RX, and dSA−RX were prepared by mixing desired amounts of the stock solutions. Three different mole ratios of dPA or dSA to each RX were used: 3:1, 1:1, and 1:3. A measured volume of fatty acid or alkyl halide solution or mixture was spread on the subphase surface in a dropwise manner with a Hamilton syringe, and 15 min was allowed to elapse for complete chloroform evaporation. The barriers were compressed at a speed of 5 mm/min/barrier.

Vibrational Sum Frequency Generation (*Broad Bandwidth Technology*). The broad bandwidth SFG experimental setup has been described elsewhere.[27,28] The Langmuir film balance was placed on the sample stage of the SFG system. The IR and visible beams are overlapped at the monolayer surface spatially and temporally. The generated SFG signal containing spectral information from the monolayer was detected using a monochromator−CCD detection system (Acton Research, SpectraProSP-500 monochromator with a 1200 groove/mm grating blazed at 750 nm; Roper Scientific, 1340 × 400 pixel array, LN400EB back-illuminated CCD). The SFG spectrum is polarization-dependent, where the polarization combinations used were ssp and ppp for the SFG, 800 nm, and infrared beams, respectively. The different polarization combinations more efficiently probe vibrational mode vectors perpendicular (ssp) and parallel (ppp and sps or pss, with ppp providing higher intensities) to the surface normal.

SFG spectra were obtained with a 5 min acquisition time as a function of incident infrared wavelength of dPA−BrHex 1:1 and dPA monolayers at the air−water interface at 5, 18, and 25 mN/m. SFG spectra were taken under the hold mode of the film balance. In this mode, the two barriers move to compensate for the surface pressure drop, and a constant pressure is therefore maintained. Background spectra were obtained for each sample by disrupting the temporal overlap of the beams. The background spectra were subtracted from the sample spectra, and the resulting spectra were normalized to the nonresonant signal from a GaAs crystal surface (Lambda Precision Optics, Inc.) to remove the spectral distortion caused by the energy profile of the infrared pulse.

To calibrate the SFG peak positions in the C−H stretching region, a nonresonant SFG spectrum from the GaAs crystal surface was obtained with a polystyrene film covering the infrared output port of the optical parametric amplifier. The resulting SFG spectrum containing polystyrene infrared absorption bands was used for the calibration. To calibrate the SFG peak positions in the C−D stretching region, the absorption bands of ambient CO_2 vapor were used.

Briefly, vibrational SFG is a second-order nonlinear surface-selective technique that provides vibrational spectra of molecules

(15) Gericke, A.; Hühnerfuss, H. *J. Phys. Chem.* **1993**, *97*, 12899–12908.
(16) Adamson, A. W.; Gast, A. P. *Physical Chemistry of Surfaces*, 6th ed.; Wiley: New York, 1997.
(17) Kaganer, V. M.; Möhwald, H.; Dutta, P. *Rev. Mod. Phys.* **1999**, *71*, 779–819.
(18) Dynarowicz-Latka, P.; Kita, K. *Adv. Colloid Interface Sci.* **1999**, *79*, 1–17.
(19) Thornton, J. A.; Kercher, J. P.; Riedel, T. P.; Wagner, N. L.; Cozic, J.; Holloway, J. S.; Dube', W. P.; Wolfe, G. M.; Quinn, P. K.; Middlebrook, A. M.; Alexander, B.; Brown, S. S. *Nature* **2010**, *464*, 271–274.
(20) Graedel, T. E.; Keen, W. C. *Global Biogeochem. Cycles* **1995**, *9*, 47–77.
(21) Keene, W. C.; Khalil, M. A. K.; Erickson, D. J., III; McCulloch, A.; Graedel, T. E.; Lobert, J. M.; Aucott, M. L.; Gong, S. L.; Harper, D. B.; Kleiman, G.; Midgley, P.; Moore, R. M.; Seuzaret, C.; Sturges, W. T.; Benkovitz, C. M.; Koropalov, V.; Barrie, L. A.; Li, Y. F. *J. Geophys. Res.*, [*Atmos.*] **1999**, *104*, 8429–8440.
(22) Carpenter, L. J.; Sturges, W. T.; Penkett, S. A.; Liss, P. S.; Alicke, B.; Hebestreit, K.; Platt, U. *J. Geophys. Res.* **1999**, *104*, 1679–1689.
(23) Butler, J. H. *Nature* (*London*) **2000**, *403*, 260–261.
(24) Ashizuka, Y.; Nakagawa, R.; Tobiishi, K.; Hori, T.; Iida, T. *J. Agric. Food Chem.* **2005**, *53*, 3807–3813.
(25) Faulkner, D. J. *Nat. Prod. Rep.* **2001**, *18*, 1–49.
(26) Kotterman, M.; van der Veen, I.; van Hesselingen, J.; Leonards, P.; Osinga, R.; de Boer, J. Preliminary study on the occurrence of brominated organic compounds in Dutch marine organisms. *Biom. Eng.* **2003**, *20*, 425–426.
(27) Hommel, E. L.; Ma, G.; Allen, H. C. *Anal. Lett.* **2001**, *17*, 1325.
(28) Ma, G.; Allen, H. C. *J. Phys. Chem. B* **2003**, *107*, 6343.

at interfaces. SFG is the generation of a sum frequency beam by two laser beams of different frequencies, one of fixed visible frequency (ω_{VIS}) and the other of tunable infrared frequency (ω_{IR}), overlapped at the surface sample in space and time. The frequency of the resulting SFG beam is the sum of the frequencies of the two incident beams. When the infrared frequency is resonant with a vibrational mode of an interfacial molecule, the SFG signal is enhanced. For broad bandwidth SFG, the infrared beam is comprised of an envelope of infrared wavelengths, and therefore the SFG spectrum must be deconvoluted, typically using a monochromator to disperse the SF generated wavelengths as was done here.

SFG intensity arises only from environments that lack inversion symmetry such as at interfaces. This rule makes vibrational SFG unique as a surface selective technique. The intensity of the SFG signal (I_{SFG}) is proportional to the intensities of the incident beams (infrared, I_{IR}, and visible, I_{VIS}) as shown in eq 1

$$I_{SFG} \propto |\chi^{(2)}|^2 I_{IR} I_{VIS} \quad (1)$$

where $\chi^{(2)}$ is the macroscopic second-order nonlinear susceptibility; $\chi^{(2)}$ is comprised of resonant terms ($\chi_v^{(2)}$) and a nonresonant term ($\chi_{NR}^{(2)}$), and $\chi_v^{(2)}$ is proportional to the molecular hyperpolarizability (β) of that vibration, to the number density, and to the molecular orientation. A detailed description of the vibrational SFG process can be found in the literature.[29−31]

IRRAS. IRRAS spectra were obtained using a PerkinElmer Spectrum 100 FTIR spectrometer equipped with a nitrogen-cooled MCT (mercury cadmium telluride) detector. Two 2 in. diameter gold mirrors were positioned apart on a breadboard in the FTIR chamber to direct the IR beam to and from the air−aqueous interface with a 40° angle of incidence with respect to the surface normal. The Langmuir film balance was placed on the breadboard in the FTIR chamber. Spectra were collected at a resolution of 4 cm^{-1} and averaged over 300 scans. A single beam spectrum of a pure water subphase was used as the background spectrum. IRRAS spectra of pure dPA and pure dSA were collected at the condensed phase (25 mN/m), whereas IRRAS spectra of mixtures were collected at 1, 5, 15, and 25 mN/m. All spectra were collected with unpolarized light. IRRAS spectra are presented as reflection−absorbance (RA) spectra, i.e., reflectance−absorbance = $-\log(R/R_0)$, where R is the IR reflectivity of the monolayer-covered surface and R_0 is the IR reflectivity of the bare water subphase. Reflectivity of an interface, as described by the Fresnel equations of reflection, is a function of the refractive index of the medium, the angle of the incident IR beam and its polarization, and the wavelength of light. A detailed description of the Fresnel equations and the RA for different angles of incidence and polarizations can be found elsewhere.[32,33] For methylene vibrations, R increases with the angle of incidence with s polarization. RA_s band intensities decrease with increasing the angle of incidence and are negative at all the incident angles. Hence, using s-polarized light, IRRAS spectra show negative peaks. On the other hand, R_p decreases to zero at the Brewster angle and increases again after passing the Brewster angle toward the surface normal. The Brewster angle for this interface is 53°. It has been shown that angles between 30° and 45° and between 70° and 80° provide good S/N.[34] Generally speaking, the optimal angle range of incidence for monolayers on water is 0−40° for transitions moments that are perpendicular to the surface normal when unpolarized radiation is used.[35] Here, a 40° angle was used.

BAM Imaging. A home-built BAM was used for imaging the monolayer film morphology from monolayers formed utilizing the same KSV minitrough used in the isotherm studies. The BAM light source (HeNe at 632.8 nm and 17 mW) is positioned at 53°, the Brewster angle for neat water. Monolayers were compressed at a rate of 5 mm/min as mentioned above. A 512 × 512 pixel-CCD camera (Andor, model DV 412) is used to acquire BAM images in real time. An acquisition time of 0.018 s and a delay of 8.923 s for the CCD to process the image were used. The principle of BAM has been describe elsewhere.[14,36] Briefly, when an air−water interface is irradiated with p-polarized light precisely at the Brewster angle (eq 2), no light is reflected from the interface.

$$\tan[\Theta_B] = \frac{\eta_2}{\eta_1} \quad (2)$$

Equation 2 shows that the Brewster angle is determined by the refractive index of air (η_1) and water (η_2) for an air−water interface. If an air−water interface is illuminated with p-polarized light at the air−water Brewster angle, a black background will be observed in the image. The addition of a Langmuir monolayer modifies the refractive index of the interface, and some light is reflected and displayed in the image, which allows the visualization of the monolayer morphology. Spatial resolution R was determined by using eq 3.

$$R = \frac{1.22\lambda}{NA} \quad (3)$$

The wavelength of the source λ corresponds to 632.8 nm and the numerical aperture (NA) of the objective lens to 0.35. R was then determined to be 2.2 μm and was confirmed by the observation of two peak intensities separated by ~2 μm in our BAM images.

Results and Discussion

Surface Pressure−Area Isotherms. Surface pressure−area isotherms were obtained after spreading the pure compound solutions on a pure water subphase. Figure 1 shows the isotherms of pure dPA (1a-1; Figure 1a, isotherm 1), dSA (Figure 1d-1), BrPent (Figure 1a-5), BrHex (Figure 1b-5), and ClHex (Figure 1c-5) films. Surface pressure−area isotherm measurements describe the phase behavior of Langmuir monolayers.[8] BrPent, BrHex, and ClHex isotherms show a constant surface pressure of zero, indicating that the alkyl halides do not form monolayers at the air−water interface as expected.[8] dPA and dSA isotherms exhibit two-dimensional states that are in good agreement with PA and SA isotherms reported previously.[8,37] The shape of the isotherms and regions of constant slope correspond to different phases. The observed isotherm regions have previously been assigned to the gas-tilted condensed (G-TC) coexistence region, tilted condensed (TC), untilted condensed (UC), and collapsed phases.[9,10,17] At 0 mN/m, the G phase is in coexistence with the TC phase as evidenced from our BAM images and is discussed below in the BAM Results section.

In Figure 1, the surface pressure of the dPA (Figure 1a-1) and dSA (Figure 1d-1) monolayers start to increase at 26 and 24 $Å^2$/molecule, respectively, indicating that the surface organization of the dPA and the dSA monolayers changes from a G-TC coexistence phase to a TC phase. The isotherms show a kink at 25 mN/m for dPA and 27 mN/m for dSA, indicating a second-order phase transition from the TC phase to the UC phase.[17] Film

(29) Hirose, C.; Akamatsu, N.; Domen, K. J. *J. Chem. Phys.* **1992**, *96*, 997–1004.
(30) Lambert, A. G.; Davies, P. B.; Neivandt, D. J. *Appl. Spectrosc. Rev.* **2005**, *40*, 103–145.
(31) Shen, Y. R. *The Principles of Nonlinear Optics*; Wiley: New York, 1984.
(32) Gericke, A.; Michailov, A. V.; Hühnerfuss, H. *Vib. Spectrosc.* **1993**, *4*, 335–348.
(33) Fina, L. J.; Tung, Y.-S. *Appl. Spectrosc.* **1991**, *45*, 986–992.
(34) Mendelsohn, R.; Brauner, J. W.; Gericke, A. *Annu. Rev. Phys. Chem.* **1995**, *46*, 305–334.
(35) Dluhy, R. A. *J. Phys. Chem.* **1986**, *90*, 1373–1379.
(36) Honig, D.; Mobius, D. *J. Phys. Chem.* **1991**, *95*, 4590–4592.
(37) Nutting, G. C.; Harkins, W. D. *J. Am. Chem. Soc.* **1939**, *61*, 1182.

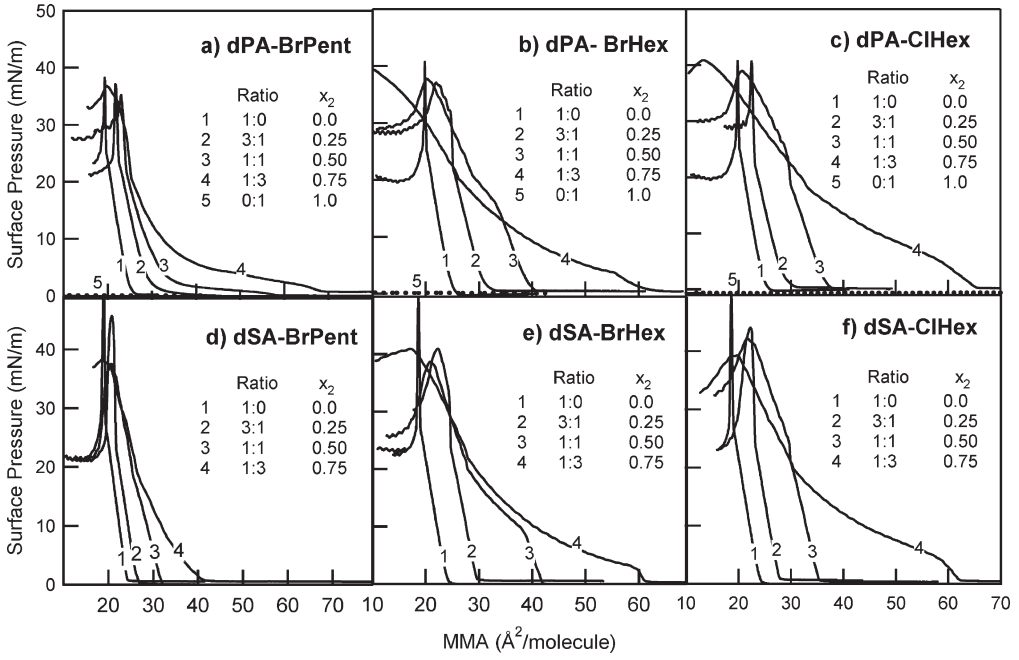

Figure 1. Surface pressure−area per fatty acid molecule isotherms of mixed monolayers at different ratios of (a) dPA−BrPent, (b) dPA−BrHex, (c) dPA−ClHex, (d) dSA−BrPent, (e) dSA−BrHex, and (f) dSA−ClHex. Mean molecular areas (MMA) of the mixed monolayers are in terms of number of fatty acid (dPA or dSA) molecules spread.

collapse occurs at 40 mN/m for dPA and at 50 mN/m for dSA. Also observed, the dSA isotherm lies to the left of the dPA isotherm. Nutting and Harkins[37] showed that the molecular area of the condensed phase decreases with the length of the hydrocarbon chain, resulting from the van der Waals energy increases with the length of the hydrocarbon chain.

As mentioned in the Introduction, the first step of this investigation was to determine the minimum alkyl chain length of alkyl halides to be incorporated into a fatty acid monolayer at the air−water interface as observed by a change in the isotherm relative to that of the pure fatty acid. Incorporation of the shorter chain 1-bromoalkanes, C_4 to C_{10}, was not observed. From the longer chain 1-bromoalkanes, BrPent and BrHex in 1:1 mixtures were observed to incorporate. A minimum of 15 carbons is needed to incorporate. However, this result does not mean that such bromoalkanes will form miscible mixed monolayers.

In addition to the bromoalkanes, incorporation studies of C_{15} and C_{16} alkanes were completed. It was observed that pentadecane and hexadecane, contrary to the corresponding bromoalkanes, do not incorporate into fatty acid monolayers as shown by an unchanged isotherm relative to that of the pure fatty acid. The halogen headgroup of a bromoalkane is not as polar compared to the COOH of a fatty acid (dPA and dSA). However, the C−Br bond of a bromoalkane is slightly more polar than the C−H bond of an alkane.[38] Thus, a C−Br bond is more likely to associate with water molecules than a terminal C−H bond of an alkane. These intermolecular forces only partially explain the observed incorporation into the monolayer since chain length is apparently more important than the dipole−dipole interactions of C−Br with surface water molecules.

C_{15}, C_{16} Alkyl Halides and dPA Mixed Monolayers. Figure 1a−c shows the surface pressure−area isotherms of dPA−BrPent, dPA−BrHex, and dPA−ClHex mixed monolayers with mole ratios of 3:1, 1:1, and 1:3 in addition to the pure compounds. If there was no incorporation of the alkyl halide, one would expect to see the isotherms of the mixed monolayer overlapped onto the pure fatty acid isotherm. The first obvious feature in Figure 1a−c is the shift of the pure dPA isotherm to larger areas upon addition of BrPent, BrHex, and ClHex, which suggests incorporation of the respective alkyl halide into the dPA monolayer. This is more evident at low surface pressures, whereas at high surface pressures the isotherms become slightly closer to the pure dPA isotherm in most cases. The increase in MMA represents the area occupied by the alkyl halides. BrPent contributes with a MMA of 33 Å^2/molecule, BrHex with 16 Å^2/molecule, and ClHex with 13 Å^2/molecule at 0 mN/m. The MMA occupied by the alkyl halide decreases with surface pressure. MMAs of the alkyl halides would be expected to be slightly lower than that of dPA since the halide group is smaller in size than that of a carboxylic acid group. However, MMAs of alkyl halides in the mixed monolayer is considerably smaller than that of the fatty acid.

For interpretation of the mixed monolayers, we will focus on the 1:1 molar ratios since the spectroscopic studies were performed only using this ratio. The dPA−BrPent isotherm (Figure 1a-3) shows a phase that does not exist in that of the pure dPA isotherm. As the dPA−BrPent mixed monolayer is compressed, there seems to be a transition from a G to a liquid expanded (LE) phase at 57 Å^2/molecule. The dPA−BrPent isotherm lifts at 57 Å^2/molecule with a very small slope. This region corresponds to the LE phase. In the LE phase, the hydrophobic chains of the molecules are thought to be randomly oriented with many gauche defects, whereas in the G phase, in addition to having the hydrophobic chains randomly oriented, the molecules are on average far apart from each other. Kaganer et al.[17] defined the LE phase as the region in which molecules behave like a two-dimensional (2D) liquid where the headgroups of the molecules are translationally disordered and the chains are conformationally disordered. For all phases the polar head groups are submerged in the aqueous subphase.[8] As the monolayer is compressed further to 34 Å^2/molecule and a surface

(38) Harper, K.; Minofar, B.; Sierra-Hernandez, M. R.; Casillas-Ituarte, N. N.; Roeselova, M.; Allen, H. C. *J. Phys. Chem. A* **2009**, *113*, 2015–2024.

pressure of 3 mN/m, the TC transition occurs. The slope of the curve in the TC phase is slightly smaller than that of the pure dPA. This suggests that some BrPent molecules are being squeezed out of the dPA monolayer.[39] The kink transition characteristic of dPA decreases from 25 to 22 mN/m in the dPA−BrPent 1:1 mixed isotherm. The dPA−BrPent 1:1 film collapses at a surface pressure of 35 mN/m, which is lower than the collapse pressure of pure dPA. The collapse occurs at an MMA of 23 Å^2/molecule, whereas the dPA monolayer collapses at 20 Å^2/molecule. This difference suggests that even though some BrPent molecules are squeezed out of the dPA monolayer at low surface pressure, the film still contains both dPA and BrPent molecules.

The addition of BrHex (Figure 1b) and ClHex (Figure 1c) shifts the isotherm of pure dPA to larger areas at low surface pressures. BrHex has a greater effect than ClHex at low surface pressures. However, at high surface pressure ClHex seems to have a slightly greater effect than BrHex. Previously, Gonçalves da Silva et al.[6] showed similar effects of both BrHex and ClHex on heptadecanoic acid, whose alkyl chain is one carbon longer than that of dPA.

The dPA−BrHex 1:1 isotherm lifts at 40 Å^2/molecule, whereas the dPA−ClHex 1:1 isotherm lifts at 37 Å^2/molecule. The difference between dPA−BrHex and dPA−ClHex lift-off values can be partially explained by the difference in size of the halogen atoms where bromine is larger than chlorine, Br covalent radius is 120 pm, and Cl is 102 pm.[40] The surface pressure of both dPA−BrHex and dPA−ClHex isotherms rises significantly after the lift-off. This region corresponds to the LC phase. Yet, the slopes of the LC phases in the mixed isotherms are smaller than that of the pure dPA.

The dPA−BrHex isotherm shows two collapse pressures. The initial collapse pressure appears at 16 mN/m, while the final collapse pressure at 37 mN/m is similar to that of pure dPA. This initial collapse pressure is attributed to the squeezing out of some BrHex molecules from the dPA monolayer as is discussed further with respect to the BAM images below. As the dPA−BrHex mixed monolayer is compressed further after the initial collapse pressure, there is an initial decrease in the slope of the isotherm, which suggests additional BrHex molecules are squeezed out. At the final collapse pressure, the dPA−BrHex isotherm is slightly shifted to higher MMA relative to that of the pure dPA, indicating that a fraction of the BrHex molecules continue to be incorporated in the monolayer at this surface pressure.

Collapse pressure is defined as the highest pressure to which a monolayer cannot be further compressed without destabilizing the 2D nature of the monolayer and yielding 3D structures due to the expulsion of molecules.[8,41] Collapse pressure has been used as a proof of miscibility or immiscibility of the components in a mixed monolayer at the air−water interface. When two fatty acids with different collapse pressures mix in a monolayer, the resulting isotherm might show a plateau at a pressure corresponding to the collapse pressure of the more fluid component (the component with the lowest collapse pressure) and a final collapse pressure similar to that of the more rigid component (the component with the highest surface pressure).[5,6,41] Thus, if the resulting isotherm of a mixed monolayer exhibits two distinct collapse pressures (initial and final), the different components of the monolayer have been identified as immiscible. On the other hand, if the resulting isotherm shows only one collapse pressure, the components are thought to form a homogeneous mixed monolayer. Here, even though two collapse pressures are observed, the isotherms are more complicated, and partial miscibility is suggested.

The isotherm obtained for the dPA−ClHex 1:1 monolayer (Figure 1c-3) also shows two collapse pressures. The initial collapse pressure appears at higher surface pressures for the dPA-ClHex monolayer (19 mN/m) than for the dPA−BrHex system (16 mN/m). Contrary to the dPA−BrHex isotherm, the dPA−ClHex isotherm does not show a plateau upon further compression. However, the slope of the curve decreases similarly to the dPA−BrHex, suggesting that ClHex molecules are being squeezed out of the dPA monolayer. The monolayer does not collapse exactly at the collapse pressure of the pure dPA, which suggests that the mixed monolayer continues to retain some of the ClHex molecules prior to and during the final collapse.

C_{15}, C_{16} Alkyl Halides and dSA Mixed Monolayers. Figure 1d-f shows the surface pressure−area isotherms of dSA−BrPent, dSA−BrHex, and dSA−ClHex mixed monolayers on a pure water subphase with mole ratios of 3:1, 1:1, and 1:3. Similar to the effect on dPA, addition of BrPent, BrHex, and ClHex shifts the pure dSA isotherm to larger areas, suggesting incorporation of the correspondent alkyl halide into the dSA monolayer.

For the mixed dSA−BrPent 1:1 monolayer, the surface pressure−area isotherm (Figure 1d-3) consists of the same distinct regions from the pure dSA isotherm, TC and UC phases. The isotherm curve for this mixed monolayer is parallel to the pure dSA isotherm. Contrary to its effect on dPA, BrPent induces a relatively small shift to larger areas at low surface pressure on dSA monolayers. Upon compression, there is a transition from a G-TC to a TC phase at 28 Å^2/molecule. This lift-off value is far smaller than the lift-off value of the dPA−BrPent isotherm (57 Å^2/molecule). The slope of the TC region in Figure 1d-3 is comparable with that of pure dSA. The kink transition characteristic of dSA decreased from 27 to ∼22.5 mN/m. As mentioned above, this kink corresponds to the transition from the TC phase to the UC phase. The dSA−BrPent film exhibits only one collapse pressure at ∼39 mN/m. The fact that the surface pressure−area isotherm of dSA−BrPent is nearly parallel to the pure dSA isotherm and that it shows only one collapse pressure suggests the formation of a homogeneously mixed monolayer and miscibility with dSA. Thus, dSA incorporates BrPent into its monolayer to form a homogeneous and an apparently stable mixed monolayer, whereas dPA, being two carbons shorter ($C_{15}D_{31}COOH$), incorporates BrPent as well, but the resulting mixed monolayer seems to organize differently with the BrPent molecules as seen from the very different phase behavior. Hence, the length of the fatty acid plays a role in the extent of BrPent incorporation. However, both dSA and dPA are miscible with BrPent as suggested from the appearance of a single collapse pressure different from that of the pure dSA and dPA films, respectively.

Incorporation of BrHex and ClHex into dSA monolayers (Figures 1e-3 and 1f-4) follows a similar trend as with the dPA monolayers. A difference observed for the BrHex and the ClHex mixed with dSA relative to the pure dSA is that their final collapse pressures are not at the same MMA. Both mixed isotherms collapse at a surface pressure ∼10 mN/m lower than, and at a MMA of ∼2 Å^2/molecule larger than, that of pure dSA. Two collapses are also observed for the mixed films with dSA as discussed above.

At collapse the isotherm pressures are shifted to larger MMA for the dSA mixtures relative to the dPA mixtures, suggesting a difference in fractional composition. This could be due to the longer chain of dSA molecules which can favor lateral attraction with the chains of the alkyl halides, thereby more efficiently

(39) Ilharco, L. M.; Garcia, A. R.; Fidalgo, A. M.; Barros, R.; Vale, A. F.; Lopes da Silva, J.; Gonçalves da Silva, A. M. *Langmuir* **1995**, *11*, 2745–2750.
(40) Cordero, B.; Gomez, V.; Platero-Prats, A. E.; Reves, M.; Echeverria, J.; Cremades, E.; Barragan, F.; Alvarez, S. *Dalton Trans.* **2008**, 2832–2838.
(41) Lee, K. Y. C. *Annu. Rev. Phys. Chem.* **2008**, *59*, 771–791.

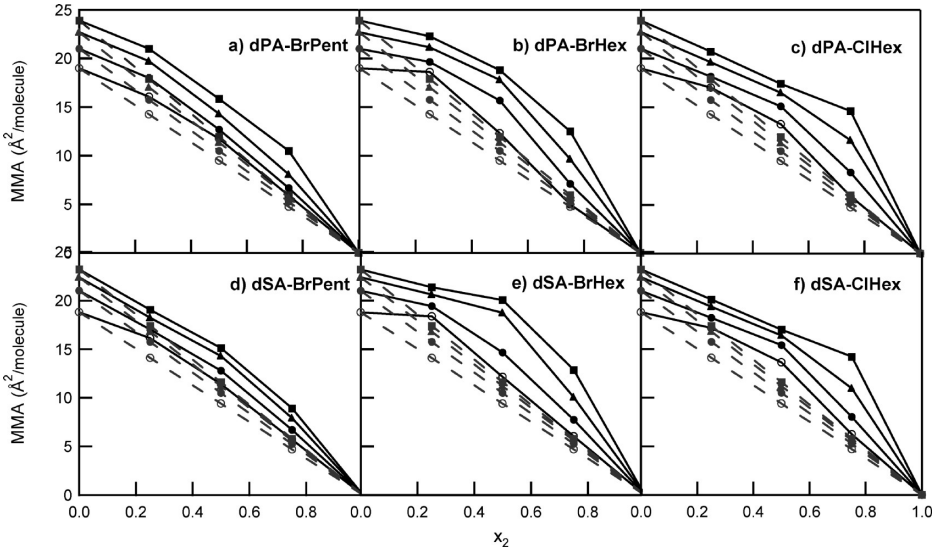

Figure 2. Mean molecular area (MMA) of dPA and dSA mixed monolayers as a function of the alkyl halide molar fraction (x_2) at various surface pressures (■, 5 mN/m; ▲,10 mN/m; ●, 18 mN/m; ○, 30 mN/m). Experimental values (——); ideal values (- - -).

retaining the alkyl halide in the film. One can also define this interaction as an indicator for miscibility.

Analysis of Figure 1 suggests that BrPent, BrHex, and ClHex at 1:1 molar ratios are miscible with dPA and dSA, respectively. To further understand the miscibility of the RX molecules investigated here, we performed surface pressure−area isotherms at different mole ratios (Figure 1) and an MMA analysis (Figure 2). Figure 2 shows the experimental and ideal MMA as a function of alkyl halide mole fraction at different surface pressures for dPA and dSA mixed monolayers. Deviations from ideality provide evidence for partial miscibility in a mixed monolayer. From this analysis, a partial miscibility between the alkyl halides and the fatty acids is concluded although the miscibility decreased with increasing surface pressure. Therefore, the extent of miscibility is dependent on concentration within the monolayer and surface pressure.

SFG Spectra. The normalized ssp and ppp SFG spectra of dPA and of the mixture dPA-BrHex 1:1 at the air−water interface at 5, 18, and 25 mN/m are shown in Figures 3 and 4, respectively. The ssp spectra taken in the C−D region to probe the dPA chains are shown in Figure 3a,b. The peaks present in the pure dPA (Figure 3a) spectra are attributed to the CD_3 symmetric stretch (ss; 2070 cm^{-1}), the CD_3 Fermi resonance (FR; 2125 cm^{-1}), and the CD_3 asymmetric stretch (as; ~2221 cm^{-1}).[9,42] The ppp-polarized spectral peak in Figure 4a,b is assigned to the CD_3-as (~2218 cm^{-1}). (Note that interference terms cause the apparent peak positions to sometimes shift relative to their true positions.[11,42]) The dPA−BrHex SFG spectra (Figure 3b) are qualitatively similar to that of pure dPA. This is also true for the ppp SFG spectra shown in Figure 4a,b where only the methyl peaks are observed for the dPA and the BrHex. The appearance of dPA and BrHex peaks is confirmation that the BrHex molecules exist in the dPA monolayer although it does not prove miscibility.

From Figures 3a,b and 4a,b, the square root of the increase in ssp and ppp SF intensity with surface pressure should be proportional to the increase in dPA molecules (eq 1). These values are plotted in Figure 5. As the monolayer is compressed, dPA molecules become more closely packed, which results in more dPA per unit area probed. Since the dPA orientation changes in the

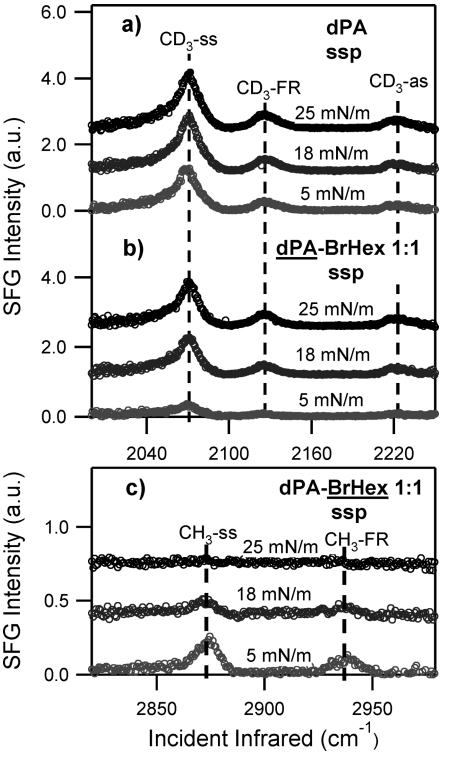

Figure 3. ssp SFG spectra probing dPA molecules in the CD stretching region of (a) pure dPA and (b) the mixture dPA−BrHex 1:1 and probing the BrHex molecules in the mixture dPA−BrHex 1:1 (c).

TC phase to the UC phase[43,44] and the dPA chains are in an all-trans configuration, the square root of the intensity will slightly overestimate the number density (Supporting Information). It is also observed from Figures 3b and 4b that SF intensities are lower for the dPA−BrHex mixed monolayer than for the pure dPA monolayer. This is more evident at low surface pressures,

(42) Yang, C. S.-C.; Richter, L. J.; Stephenson, J. C.; Briggman, K. A. *Langmuir* **2002**, *18*, 7549–7556.

(43) Weidemann, G.; Brezesinski, G.; Vollhardt, D.; Bringezu, F.; de Meijere, K.; Mohwald, H. *J. Phys. Chem. B* **1998**, *102*, 148–153.

(44) Lee, K. Y. C.; Gopal, A.; von Nahmen, A.; Zasadzinski, J. A.; Majewski, J.; Smith, G. S.; Howes, P. B.; Kjaer, K. *J. Chem. Phys.* **2002**, *116*, 774.

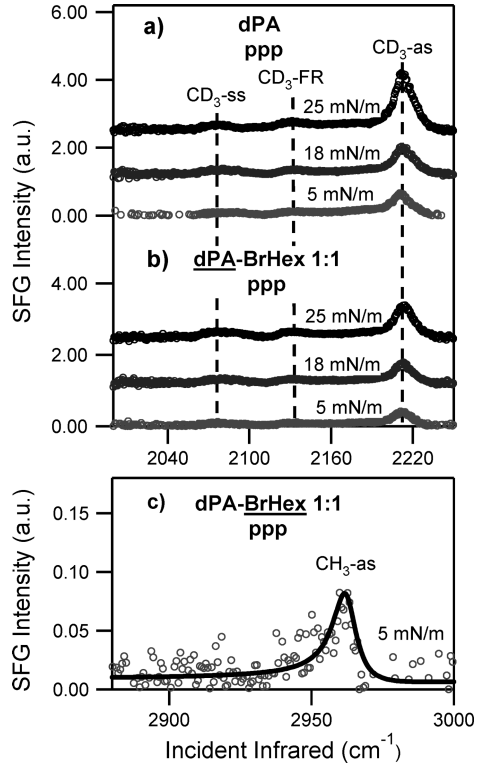

Figure 4. ppp BBSFG spectra probing dPA molecules in the CD stretching region of (a) pure dPA and (b) the mixture dPA−BrHex 1:1 and probing the BrHex molecules in the mixture dPA−BrHex 1:1 at 5 mN/m (c).

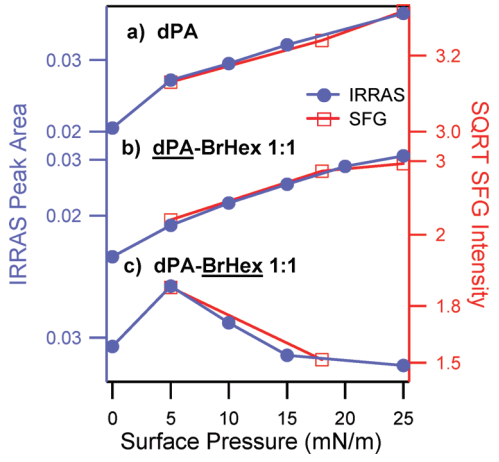

Figure 5. Comparison of the square root (SQRT) of the CD_3-ss peak intensity obtained by SFG and the CD_2-ss peak area obtained by IRRAS of dPA (a) and dPA−BrHex 1:1 (b). Panel c is the comparison of the SQRT of the CH_3-ss peak intensity obtained by SFG and the CH_2-ss peak area obtained by IRRAS of dPA−BrHex 1:1.

suggesting that at low surface pressures BrHex molecules are incorporated into the mixed monolayer.

BrHex molecules were probed by acquiring ssp and ppp SFG spectra in the C−H stretching region of the mixed monolayer of dPA−BrHex 1:1 (Figures 3c and 4c, respectively). The two main peaks observed in Figure 3c are attributed to the CH_3-ss (2872 cm^{-1}) and the CH_3-FR (2939 cm^{-1}). For Figure 4c, the

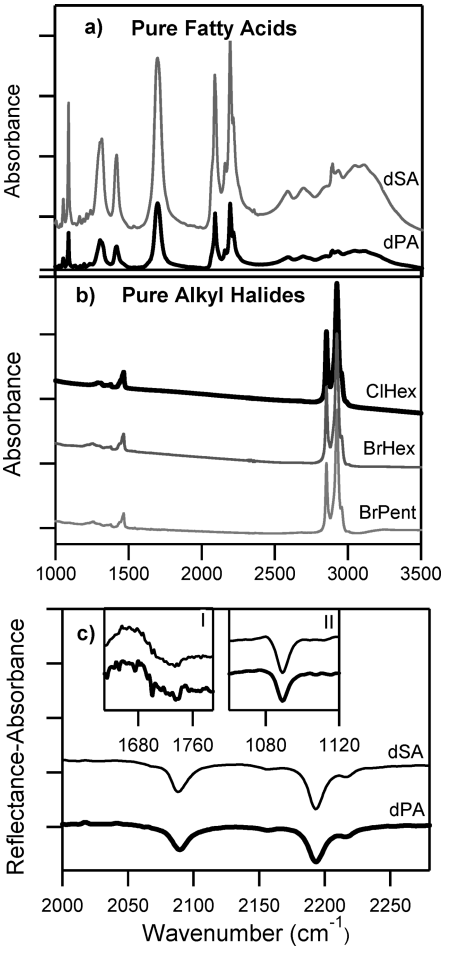

Figure 6. Absorbance infrared spectra of (a) pure fatty acids and (b) pure alkyl halides and (c) IRRAS spectra of pure fatty acids on a water subphase at 25 mN/m; spectra were collected with unpolarized light. Inset I: C=O region. Inset II: CD_2 scissoring mode (1088 cm^{-1}).

single peak is assigned to the CH_3-as (~2963 cm^{-1}).[45−47] Contrary to the CD peaks from dPA molecules, the intensity of the CH peaks decreases as the monolayer is compressed. This can be interpreted as disordering of the BrHex molecules in the dPA monolayer, although additional investigations to further understand this intensity decrease for the BrHex are discussed below.

IRRAS Spectroscopy. IRRAS spectra were obtained for two different systems, dPA−BrHex (3:1 and 1:1) and dSA−BrHex (3:1 and 1:1), to further elucidate conformational order, incorporation, and BrHex number density. Because of differences in selection rules, IRRAS is sensitive to different vibrational modes of the fatty acids and alkyl halides compared to SFG, and it is therefore complementary to the SFG study above. Spectra of amphiphilic molecules show clear reflectance−absorbance peaks from the methylene groups of alkyl chains. The positions of the CH_2-ss and CH_2-as peaks reveal the relative number of trans and gauche conformers, while the peak heights and areas are sensitive to the packing density and the tilt angle of the chains.

As control experiments, infrared transmission spectroscopy of the pure fatty acids (dPA and dSA) and the alkyl halides (BrPent, BrHex, and ClHex) were obtained and are shown in parts a and b

(45) Wang, H.-F.; Gan, W.; Lu, R.; Rao, Y.; Wu, B.-H. *Int. Rev. Phys. Chem.* **2005**, *24*, 191–256.

(46) Van Loon, L. L.; Minor, R. N.; Allen, H. C. *J. Phys. Chem. A* **2007**, *111*, 7338–7346.

(47) Xu, M.; Liu, D.; Allen, H. C. *Environ. Sci. Technol.* **2006**, *40*, 1566–1572.

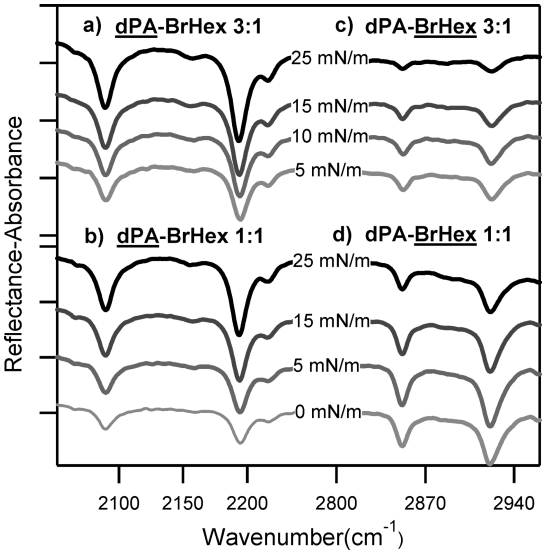

Figure 7. IRRAS spectra of the dPA−BrHex mixture at 1, 5, 15, and 25 mN/m obtained with unpolarized light. Panels a (dPA−BrHex 3:1) and b (dPA−BrHex 1:1) show the CD stretching region, which represents the dPA component in the monolayer. Panels c (dPA−BrHex 3:1) and d (dPA−BrHex 1:1) show the CH stretching region, which represents the BrHex component in the monolayer.

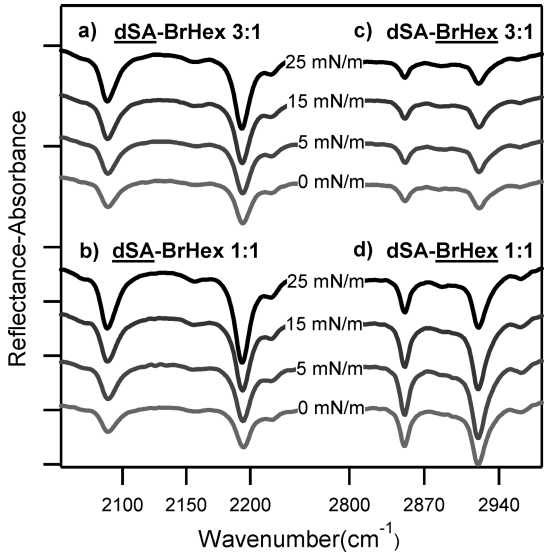

Figure 8. IRRAS spectra of the dSA−BrHex mixture at 1, 5, 15, and 25 mN/m obtained with unpolarized light. Panels a (dSA−BrHex 3:1) and b (dSA−BrHex 1:1) show the CD stretching region, which represents the dPA component in the monolayer. Panels c (dSA−BrHex 3:1) and d (dSA−BrHex 1:1) show the CH stretching region, which represents the BrHex component in the monolayer.

of Figure 6, respectively. At 2087 and 2193 cm^{-1} in Figure 6a, the fatty acid CD_2-ss and CD_2-as modes are observed, and the peak at 1699 cm^{-1} corresponds to the C=O stretching vibration. In Figure 6b, the alkyl halide peaks at 2852 and 2923 cm^{-1} correspond to the CH_2-ss and CH_2-as modes, respectively.

In Figure 6c the IRRAS spectra of dPA and dSA monolayers on a water subphase at 25 mN/m are shown. Negative peaks are observed as expected. Both spectra show the CD_2-ss at 2087 cm^{-1}, the CD_2-as modes at 2193 cm^{-1}, and the CD_3-as at 2216 cm^{-1}. Such frequencies for CD_2 vibrations are characteristic of transition moments perpendicular to the axis of an all-trans chain,[34] consistent with our interpretation from the SFG spectra above from the pure dPA monolayer in the UC phase. The IRRAS spectra also show structure around 1700 cm^{-1} formed by an upward-oriented band at 1650 cm^{-1} and a downward-oriented band at 1720 cm^{-1}(Figure 6c, inset I). The 1650 cm^{-1} band is associated with the bending mode of the water, whereas the 1720 cm^{-1} band is assigned to C=O stretching vibrations. The 1720 cm^{-1} band is formed by three peaks. Following assignments made by Gericke and Hühnerfuss[15] for stearic acid, the peak at 1703 cm^{-1} is due to a doubly hydrated carbonyl group, the 1720 cm^{-1} peak is from the monohydrated state, and the 1737 cm^{-1} peak is due to the nonhydrated carbonyl group.[15,48] A 1088 cm^{-1} peak is observed (Figure 6c, inset II) and is assigned to the CD_2 scissoring mode.[34,49] The presence of this mode suggests a hexagonal or triclinic phase.[34,49,50]

IRRAS spectra of the dPA−BrHex 3:1 and 1:1 mixture are shown in Figure 7 and of dSA−BrHex 3:1 and 1:1 in Figure 8 at different surface pressures. In addition to the CD peaks observed at 2087, 2193, and 2192 cm^{-1}, CH peaks from the BrHex are observed at 2852 and 2923 cm^{-1}, which confirms that the BrHex molecules exist in the fatty acid monolayer as was also indicated by the SFG spectra from the dPA mixtures above. It is observed that as the surface pressure increases, the reflectance−absorbance intensity of the CD peaks increases. This is reasonable since upon compression molecules become closer, and therefore there are more molecules per unit area. On the other hand, CH peaks, which represent the alkyl halide molecules, increase only from 0 to 5 mN/m and then decrease gradually with surface pressure. The observed decrease in the IRRAS intensity at high surface pressure could be due to a decrease in number density; however, it is also consistent with a stable surface number density because reflectance−absorbance intensities depend on the orientation of a particular transition moment in the *x*, *y*, and *z* directions. Moreover, the angle of the incident light will preferentially bias certain orientations, in particular for a molecule that is oriented perpendicular to the surface plane (for the CH_2-ss). To explain further, radiation that is s-polarized has components only in the *y* direction as defined in our system, whereas p-polarized radiation has components in both *x* and *z* directions.[32,34] For this study due to the geometry of the experiment, the unpolarized radiation is dominated by s-polarized radiation, and therefore if the molecular conformation changes and the surface number density does not change, IRRAS intensity may be subject to change. Beyond 5 mN/m, our spectra suggest that BrHex molecules are squeezed out of the dPA monolayer, and their conformation is changed. SFG spectra in Figure 3c at 25 mN/m show the absence of CH peaks. Because of the SFG lack of inversion symmetry rule, the CH peak absence (below our SFG detection limits) indicates that BrHex molecules are not ordered.

These results, IRRAS and SFG, are also consistent with the surface-pressure area isotherms and the area analysis that suggests that the alkyl halide molecules, although incorporated throughout the compression, are being squeezed out of the fatty acid monolayers and are becoming disordered as the compression proceeds. This is further shown in Figure 5, where the CD_2-as and CH_2-ss IRRAS intensity is plotted with the CD_3-ss and CH_3-ss SFG of dPA and BrHex, respectively.

We also conclude from the IRRAS spectra that the alkyl chains of both fatty acids (dPA and dSA) increase in ordering with and

(48) Brauner, J. W.; Flach, C. R.; Xu, Z.; Bi, X.; Lewis, R. N. A. H.; McElhaney, R. N.; Gericke, A.; Mendelsohn, R. *J. Phys. Chem. B* **2003**, *107*, 7202–7211.
(49) Snyder, R. G.; Liang, G. L.; Strauss, H. L.; Mendelsohn, R. *Biophys. J.* **1996**, *71*, 3186–3198.
(50) Sun, W.-J.; Tristram-Nagle, S.; Suter, R. M.; Nagle, J. F. *Biochim. Biophys. Acta* **1996**, *1279*, 17–24.

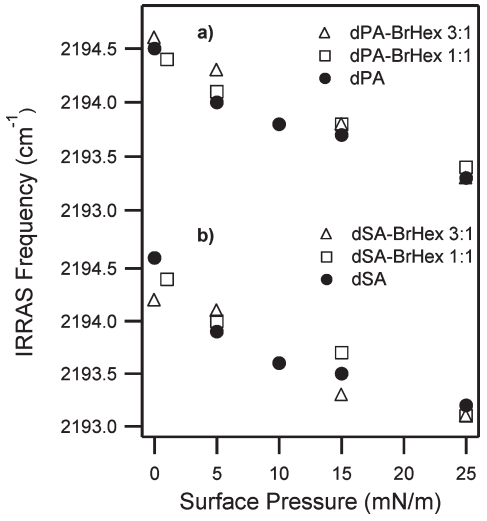

Figure 9. Fatty acid frequency dependence of the CD_2-as on the surface pressure of (a) dPA and dPA−BrHex mixtures and of (b) dSA and dSA−BrHex mixtures.

without the BrHex as shown in Figure 9. The IRRAS BrHex frequency data did not show any change in the mixed monolayers, which suggests that there is no discernible intermolecular interaction between the dPA and the BrHex alkyl chains during compression.

Even though we observe a small red-shifting of the dPA and dSA IRRAS CD_2-as frequencies as presented in Figure 9, the spectral range of the frequencies[34] supports the conclusion of predominately all-trans conformations for dPA and dSA at all surface pressures. This is also supported by the lack of SFG CD_2 peak intensities as shown in Figure 3 and as discussed above. The all-trans conformation of the fatty acids chains makes the dPA and dSA rigid molecules in their monolayers. It has been suggested that PA being a rigid molecule hinders the rotational isomerization of DPPC (dipalmitoylphosphatidylcholine) chains reducing the number of gauche defects, which forces DPPC molecules into a condensed phase.[9] In this investigation, the dPA and dSA effect on alkyl halide molecules may be similar to that on DPPC, forcing the alkyl halides into a condensed phase. As was mentioned above, contrary to their corresponding alkyl halides, alkanes do not incorporate into the fatty acid monolayers. Thus, in addition to having a relatively rigid fatty acid such as PA or SA, a headgroup that interacts with water is of great importance for formation of the monolayer.

Also, IRRAS spectra show that BrHex molecules are squeezed out with increase in surface pressure in accordance with our analysis of the isotherms and the MMAs as is suggested from Figure 5 as well, in addition to the spectroscopy results. Fatty acid molecules force alkyl halide molecules into a liquid or condensed phase in the mixed monolayer; however, the interactions of the fatty acid chains with the RX chains and the halogen with water molecules are weak, and therefore as the surface pressure increases, alkyl halide molecules are not retained in the monolayer. Contrary to the carboxylic acid headgroup that acts as an H-bond donor and acceptor during hydrogen bond formation with interfacial water molecules, a halogen can act only as an H-bond acceptor.[38]

The C=O stretching vibration band of both dPA−BrHex 1:1 and dSA−BrHex 3:1 shows the three peaks at 1737, 1720, and 1703 cm^{-1} (spectra not shown). The spectra also show the CD_2 scissoring mode at 1088 cm^{-1}. Comparing the spectra of the mixed monolayers with those of pure dPA and dSA, no frequency

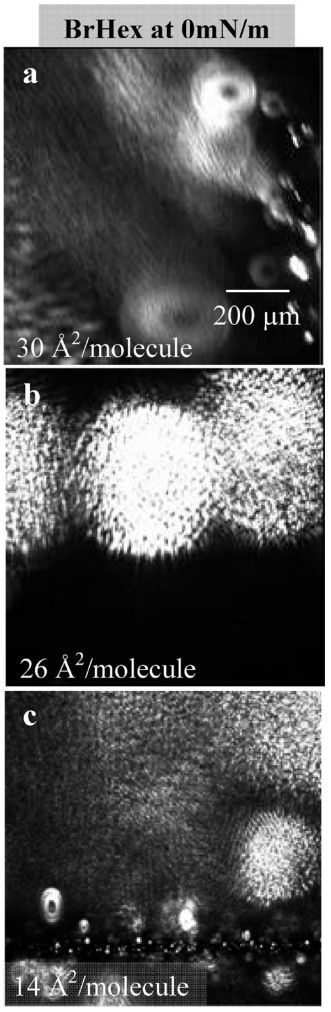

Figure 10. BAM images for pure BrHex at different MMAs.

changes are observed, which suggests that the dPA and dSA conformation is not altered by the presence of BrHex. Ilharco et al.[39] investigated mixed Langmuir−Blodgett films of cadmium heptadecanoate with chloro/bromohexadecane on CaF_2 substrates by transmission IR. They observed a frequency shift of the COO^--as (at 1535 cm^{-1}) in the presence of alkyl halides. In our IRRAS spectra, the strong absorption of water vapor hinders the low spectral region from 1400 to 1600 cm^{-1}, and therefore we were not able to observe this peak. Shifting of the COO^- peak in their studies could be indicative of miscibility of the alkyl halides and a changing environment for the fatty acid.

BAM Results. The isotherm, SFG, and IRRAS data clearly indicate that the long chain alkyl halides incorporate into mixed monolayer films of fatty acids. However, additional information can be gleaned from surface images that provide organization information on a larger scale. Therefore, BAM images were obtained.

Three BAM images of pure BrHex after an attempt to spread on the water surface at varying compression are shown in Figure 10. The images are presented noting the average MMA; however, as shown in the isotherms of Figure 1, BrHex as well as the other RX molecules do not form monolayers at the air−water interface, and therefore the surface pressure does not change with compression. As stated above, this is well-known.[8] However, BAM images of BrHex provide an interesting contrast to the fatty acid and the mixed monolayer images shown in Figures 11 and 12. At 30 MMA and 27 MMA, the largest areas per molecule imaged; it is clear that

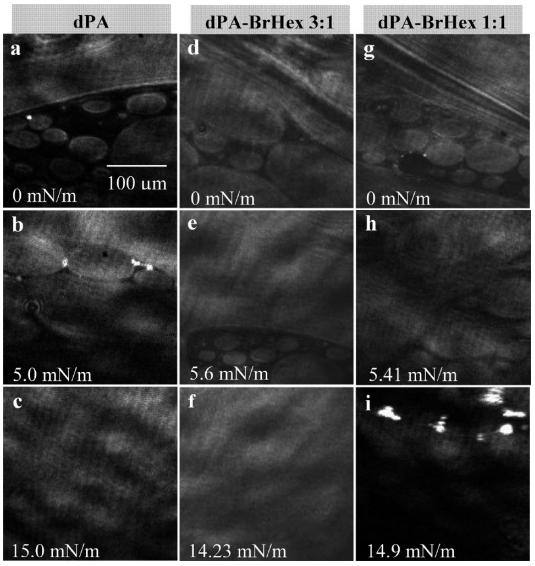

Figure 11. BAM images for pure dPA (a−c) for the mixed monolayer of dPA−BrHex 3:1 (d−f) and for the mixed monolayer of dPA-BrHex 1:1 (g−i) acquired at different surface pressures.

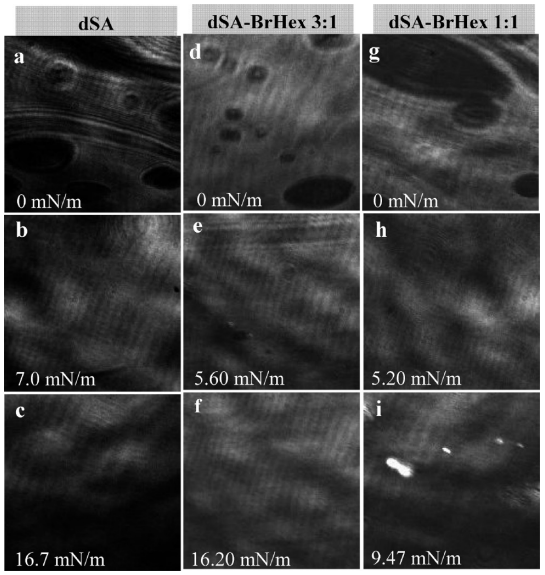

Figure 12. BAM images for pure dSA (a−c) for the mixed monolayer of dSA−BrHex 3:1 (d−f) and for the mixed monolayer of dSA−BrHex 1:1 (g−i) acquired at different surface pressures.

monolayer spreading is not taking place and that aggregates of the BrHex are formed. The weavelike features are unique to the BrHex at the surface of water. At the smallest MMA of 14 $Å^2$/molecule, the image shows larger areas of high reflectivity along with smaller and more reflective aggregates. The brightness indicates thicker films consistent with 3D structures as opposed to uniform 2D monolayer formation of dPA and dSA, as discussed below. To our knowledge, this is the first published account of BAM images of alkyl halide molecules aggregating at the surface of water.

BAM images of pure dPA and its mixture with BrHex at different surface pressures are shown in Figure 11 to elucidate the 2D morphology changes of the mixed monolayers. In Figure 11a at 0 mN/m the darker background suggests either a pure water surface or a very low density of dPA molecules consistent with a 2D dPA G phase. The condensed phase is observed as round-shaped domains, which vary in size from a few micrometers to hundreds of micrometers. Such domains show a uniform brightness, indicating a uniform surface density and orientation of the alkyl chains consistent with a TC phase. Hence, these domains at 0 mN/m are attributed to the coexistence of the G phase with the TC phase. Upon film compression, the domains become closely packed and are more similar in size as shown in Figure 11b. In Figure 10c at 15 mN/m, a homogeneous film, which corresponds to the UC phase, is observed. (The periodic changes in the background intensity are discerned more obviously in images with homogeneous surfaces and are not attributed to structural changes in the films.) The presence of a homogeneous film indicates that the alkyl chains in the dPA molecules have similar orientations and the film is of uniform thickness. These results are consistent with observations made by Qi et al.[51] and Flach et al.[52]

The surface pressure−area isotherms of dPA shift to the right when BrHex and dPA are mixed. The domains observed for pure dPA do not appear to be affected by the presence of BrHex as it is observed in the BAM images at low surface pressures in Figure 11d,e,g,h. This suggests that the BrHex molecules are incorporated in the expanded phase. As the surface pressure is increased, a homogeneous film forms (Figure 11i). However, at 17.71 mN/m for the dPA−BrHex 3:1 (data not shown) and at 14.9 mN/m for the 1:1 mixture (Figure 11f), aggregates with high reflectivity appear, similar to the small bright features observed in the BAM images of BrHex in Figure 10a,c. High reflectivity aggregates (i.e., white regions) are indicative of multilayers. Since the SFG and IRRAS results suggested that BrHex molecules are squeezed out, and from the evidence from the BrHex images, these bright aggregates are likely comprised of BrHex molecules. This is consistent with the BrHex surface pressure−area isotherm initial collapse at ~16 mN/m (Figure 1b-3), indicating some phase separation at those surface pressures.

The BAM images of dSA and its mixtures are presented in Figure 12 and are distinctly different than the dPA BAM images. Figure 12a shows the characteristic morphology of stearic acid at 0 mN/m.[53] The bright regions indicate higher densities of dSA molecules relative to the darker regions. Lee et al.[53] suggested that the gas phase forms elliptical domains and disperse in the condensed phase, as is observed in Figure 12a. Upon compression the high-density dSA domains coalesce to form a uniform film, as is observed in Figure 12b,c. In the case of dSA mixed monolayers, the same trend as with dPA is observed. The addition of BrHex does not significantly affect the dSA morphology. Figure 12d,g shows the characteristic morphology of dSA at 0 mN/m. Upon compression of the mixed monolayers, highly reflective aggregates appear at 9.47 mN/for dSA-BrHex 1:1, which is consistent with the initial collapse of its surface pressure−area isotherm (Figure 1d-3) and the squeezing out or exclusion of a fraction of the alkyl halide molecules as aggregates.

To further examine the images relative to the respective isotherms of BrHex in the fatty acids, the fractional area of the bright domains obtained from the BAM images as a function of surface pressure was plotted in Figure 13. The domain fractional areas were estimated as the ratio of the area occupied by the domains in the BAM image to the total area of the BAM image and was obtained from these images (Figures 11 and 12) in addition to previously obtained BAM images. This analysis shows that upon comparison of the pure fatty acid films to the mixed films an increase in area is occupied at surface pressures

(51) Qi, S.; Roser, S. J.; Deutsch, D.; Barker, S. A.; Craig, D. Q. M. *J. Pharm. Sci.* **2008**, *97*, 1864–1877.
(52) Flach, C. R.; Mendelsohn, R.; Rerek, M. E.; Moore, D. J. *J. Phys. Chem. B* **2000**, *104*, 2159–2165.
(53) Lee, Y. T.; Yang, Y.-C.; Shen, Y.-J. *J. Phys. Chem. B* **2005**, *109*, 4662–4667.

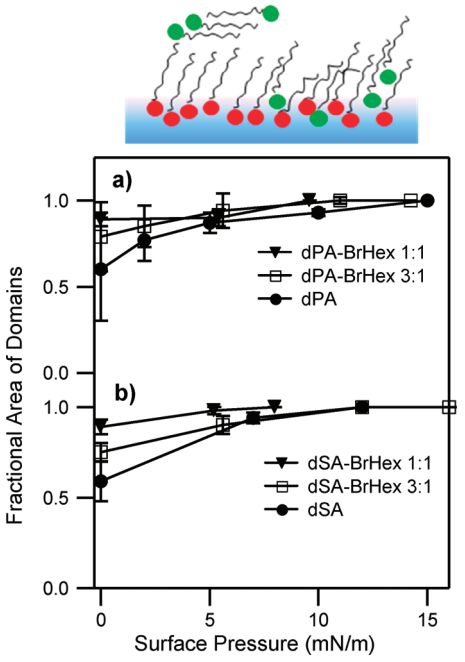

Figure 13. Fractional area of domains from the BAM images as a function of surface pressure for (a) dPA and dPA mixtures and for (b) dSA and dSA mixtures. Schematic (top illustration) suggests that at higher surface pressures the BrHex molecules (green) exist in the monolayer and are also expelled to the top of the fatty acid film (red).

Table 1. Solubilities of Some Alkyl Halides in Water[55]

bromoalkane (no. of carbons)	solubility (g/L)	bromoalkane (no. of carbons)	solubility (g/L)
C3	2.5	C6	0.037
C4	0.87	C8	0.001 67
C5	0.127	C16	0.037

below 10 mN/m, consistent with incorporation of the BrHex molecules into the monolayer. The large error bars observed for dPA at low surface pressures show that the dPA domains vary in size and are not uniformly dispersed on the subphase. This is also observed for dSA at 0 mN/m. The MMA (in terms of area per molecule in the mixed monolayer not per fatty acid molecule) information obtained from the isotherms (Figure 2) suggests that the MMA should decrease with addition of BrHex; however, the BAM images show that the domains cover larger areas. This suggests that density in the mixed monolayer domains is lower compared to that of the pure fatty acid domains. The large area covered by mixed monolayer domains suggests that the molecules are in a more expanded conformation compared with the pure fatty acid domains.

Conclusions

Mixed monolayers of fatty acids and alkyl halides at the air−water interface were studied here by the combination of four complementary techniques: Langmuir isotherm measurements, SFG, IRRAS, and BAM. Alkyl halides, in contrast to long chain fatty acids, do not form monolayers by themselves at the air−water interface; however, organization of BrHex aggregates at the surface is observed by BAM. We determined that a chain length of 15 carbons for an alkyl bromide is necessary for incorporation into dPA and dSA monolayers. Contrary to this, alkanes do not incorporate into the fatty acid monolayers, indicating that even though the halogen is not a strongly polar group it plays an important role for the incorporation alkyl halides into fatty acid monolayers. The alkyl halide molecules are squeezed out of the fatty acid monolayer at higher surface pressure, and it is highly likely that they reside on top of the fatty acid monolayer in part due to their low solubility in the water subphase and that the carboxylic group of the fatty acid molecules interacts more strongly with water molecules than with the halide of alkyl halide molecules.

With increasing surface pressure, BAM images confirm the presence of aggregates. SFG and IRRAS results also revealed that alkyl halide molecules incorporate into the dPA and dSA monolayer and, moreover, that they are not retained as surface pressure increases. For the case of the other alkyl halides tested, C4−C14, these relatively insoluble molecules (Table 1) also may reside on top of the fatty acid monolayer using a similar argument of low solubility and low hydrophilicity. For BrHex, BAM images reveal miscibility in dPA and dSA monolayers, and immiscibility at higher surface pressures as the BrHex multilayer aggregates are shown to be expelled at the first collapse pressure.

By studying the planar surface of water, this investigation provides insight into the organization of alkyl halides on fat-coated marine aerosols. Our results can be extrapolated to spherical aerosols of radius greater than or equal to 10 nm as the curvature of a 10 nm or larger droplet does not significantly affect its surface tension.[54] These results suggest that the structure of organic layers on the surface of an atmospheric aerosol is impacted by the presence of alkyl halides. These surface-active halogenated molecules do not arrange in the same way as fatty acids or other surfactant-like molecules. The halogen of an alkyl halide is not well solvated, and therefore the molecule tends to be expelled and excluded from fatty acid monolayers. It is likely that long chain alkyl halides will be present on top of a surface organic layer of atmospheric aerosols even at relatively low alkyl halide concentrations. Additionally, alkyl halides may only exist incorporated into a surface organic/surfactant film at relatively low fatty acid (or other surfactant) surface concentrations.

Acknowledgment. We thank the National Science Foundation (NSF-CHE # 0749807) for funding this work.

Supporting Information Available: Analysis of orientation angle from SFG data. This material is available free of charge via the Internet at http://pubs.acs.org.

(54) Dufour, L.; Defay, R. *Thermodynamics of Clouds*; Academic Press: New York, 1963.
(55) *CRC Handbook of Chemistry and Physics*, 91st ed.; CRC: Cleveland, OH, 2011 (Internet Version).